

Comparative Analysis of Wavelet Families in Image Compression, Featuring the Proposed New Wavelet

İbrahim ÖZ^{1*}

¹ Ankara Yıldırım Beyazıt Üniversitesi, TTO, Ayvalı Mah. Ankara, Türkiye
*¹ ibrahimoz@gazi.edu.tr

(Geliş/Received: 30/01/2024;

Kabul/Accepted: 28/03/2024)

Abstract: Image compression is fundamental to the efficient and cost-effective use of digital media, including but not limited to medical imagery, satellite images, and daily photography. Wavelet transform is one of the best methods used in compression. This study conducts a meticulous comparative analysis of various established wavelet families and introduces a novel wavelet named new wavelet for image compression (NWI), shedding light on its performance compared to well-established counterparts. This research conducts a meticulous comparative analysis of various wavelet families to assess their performance in image compression. The results show that an average compression ratio of around 75% can be achieved with a 38 dB PSNR value for all test images. The best result was achieved with the test-2 image, with a compression performance (CP) of 3312.08, using the proposed NWI wavelet. The research evaluates eight wavelet families and shows that the performance of image compression depends on both image type and selected wavelet family while keeping the coding algorithm the same for all calculations of image processing scenarios. In image compression, introducing new wavelet families, such as the NWI, can enhance performance and achieve better results.

Keywords: Wavelet, image compression, image processing, compression ratio, signal-to-noise ratio

Görüntü Sıkıştırma Dalgacık Ailelerinin Karşılaştırmalı Analizi ve Yeni bir Dalgacık Ailesi Önerisi

Öz: Görüntü sıkıştırma, tıbbi görüntülerden uydu görüntülerine ve günlük fotoğrafçılığa kadar dijital medyanın verimli ve maliyet etkili kullanımı için temel bir gerekliliktir. Dalgacık dönüşümü, görüntü sıkıştırma için kullanılan en iyi yöntemlerden biridir. Bu araştırma, en çok bilinen dalgacık ailelerinin görüntü sıkıştırma performansını çeşitli analizlerle değerlendirmiştir. İlave olarak nwi adlı yeni bir dalgacık ailesi üretilmiş ve performansı bilinen dalgacık aileleri ile karşılaştırılmıştır. Sıkıştırma Oranı (CR) ve Tepe Sinyal-Gürültü Oranı (PSNR) gibi nicel ölçüleri kullanarak, tablolar ve şekillerde sunulan sonuçlar, farklı dalgacık dönüşümlerinin performansını göstermektedir. Sonuçlar, tüm test görüntüleri için ortalama %75 sıkıştırma oranının 38 dB PSNR değeri ile elde edilebileceğini göstermektedir. En iyi sonuç, önerilen NWI dalgacığı ile test-2 görüntüsünde sıkıştırma performansı (CP) 3312,08 değeri ile elde edilmiştir. Bu çalışmada, sekiz dalgacık ailesi değerlendirilmekte ve görüntü sıkıştırma performansının hem görüntü türüne hem de seçilen dalgacık ailesine bağlı olduğu sonucu çıkmaktadır. Kodlama algoritması tüm dalgacık aileleri için aynı tutularak sadece dalgacık dönüşüm performansı analiz edilmiştir. Görüntü sıkıştırma için yeni ve etkili dalgacık ailelerinin gerçekleştirilebileceği NWI önerisinde olduğu gibi gösterilmiştir.

Anahtar kelimeler: Dalgacık, görüntü sıkıştırma, sıkıştırma oranı, sinyal gürültü oranı.

1. Introduction

The ubiquity of digital images in various domains, including social media platforms, satellite imagery, and medical imaging, has led to a surge in daily usage. However, the storage and transmission of uncompressed multimedia data, encompassing videos, photos, graphics, and audio, pose challenges due to their substantial space and bandwidth requirements. Efficient systems with sufficient memory and robust processors are essential for handling the storage and processing demands associated with such unprocessed data.

Both moving and still images are frequently broadcasted for human consumption. During viewing, imperceptible details can be selectively removed from storage to mitigate data size and reduce transmission bandwidth while maintaining a predefined image quality threshold.

Compression is pivotal in addressing these challenges, allowing videos and images to occupy less storage space and utilize minimal bandwidth during transmission without compromising perceptible image quality. Raw images generated by contemporary digital devices exhibit considerable data size and transmission rates. For instance, in high-definition image systems like HD (1920x1080 pixels), a standard image requires a 16.5 Mbyte file size. In more advanced systems such as 4KHD (3840x2160 pixels), this requirement escalates to 66 Mbyte.

The transmission and storage of image signals at exceedingly high data rates pose practical challenges. Consequently, the most viable solution is to employ compression techniques to reduce the file size and data rate

* Corresponding author: ibrahimoz@gazi.edu.tr. ORCID 0000-0003-4593-917X

to manageable levels. Digital images are compressed by removing redundant information, with three primary types of redundancy addressed [1]. **Spatial Redundancy:** In natural images, neighboring pixels often exhibit very close values. As a result, identical pixels are not individually coded; instead, the information that they share the same value is stored. The focus is on preserving the different information between closely located pixels, minimizing the need for redundant coding. **Temporal Redundancy:** In video sequences, successive frames typically have minimal changes. Regions of the frame that remain unchanged over time contribute to temporal redundancy. The information indicating that these areas are consistent with the previous frame is stored to optimize storage and transmission. Temporal redundancy reduction is particularly crucial in video compression scenarios. **Spectral Redundancy:** Image portions divided into frequency bands exhibit spectral values of closely located pixels that are very similar. These subtle details, often imperceptible to the human eye, are discarded. By doing so, the method efficiently eliminates spectral redundancy, preventing the unnecessary repetition of similar information and effectively shortening the data series representing the image information [2].

These redundancy reduction methods collectively contribute to a streamlined representation of image data, ensuring more efficient transmission and storage without compromising essential visual information.

The Discrete Wavelet Transform (DWT) is a widely utilized signal and image analysis tool. It dissects data into approximation and detail coefficients using filters, capturing localized and overall variations. The hierarchical decomposition facilitated by DWT allows for efficient data representation and compression. This transformative method finds applications in diverse fields, such as compression, noise removal, and feature extraction. Despite its proficiency in preserving crucial details, it is essential to note that DWT may introduce blocking artifacts and possess higher computational complexity when compared to simpler transforms [3].

Signal processing has seen a burgeoning interest in wavelets and wavelet transforms, marking a significant area of research. Their applications, especially in the 2D Discrete Wavelet Transform (DWT) context, have become pivotal in multimedia applications such as JPEG2000 and MPEG-4 standards, multimedia information recovery systems, and digital watermarking. The discrete mayor wavelet demonstrates remarkable effectiveness in image deblurring. Biorthogonal wavelets have been proposed to expedite the processing of geometric models, while the Fejer-korovkin wavelet exhibits a commendable response in human noise identification within multimedia applications. A novel method for enhancing image contrast, termed low dynamic range histogram equalization (LDR-HE), is introduced. This method relies on the Quantized Discrete Haar Wavelet Transform (HWT) in the frequency domain [4].

In addressing the challenges associated with separating noise from partial discharge signals, efforts have been directed towards Fourier transform, applied in the frequency or time domains. However, inherent limitations arise, as acquiring information from both time and frequency domains simultaneously proves elusive. To overcome these challenges, researchers have turned to coiflet and symlet wavelet transformations.

While the 2D DWT plays a pivotal role in multimedia applications, it comes with computational complexity, especially compared to other functions like those in the JPEG2000 standard. Consequently, many architectures have been proposed to process 2D DWT efficiently. Its application extends to enhanced ultrasonic flaw detection, and innovative structures, such as a memory-efficient 2D DWT for JPEG2000, have been put forth. This proposed structure involves a 1D column processor, internal memory, and a 1D row processor, with a primary advantage being reducing memory requirements [5].

There are numerous fields where wavelet applications find relevance, and authors have introduced various image compression techniques. These contributions have been published and shared within the academic community and among professionals.

By harnessing influential frequency bands through wavelet transform and selecting high-performance features, it is possible to detect faults in power transmission lines using ensemble learning, specifically addressing discharge faults [6]. The application of wavelet transform can be employed to address the challenge of eliminating noise arising from abrupt changes in very low frequency (VLF) signals utilized in remote sensing, which is particularly crucial for the detection of sub-ionospheric events. In industrial applications, specifically asynchronous motors, misalignment faults, including issues like loose connections and angular imbalances, can be effectively analyzed using Wavelet, transform [7].

Efficient storage and transmission of medical images are pivotal in telemedicine. The application of wavelet transform proves instrumental in achieving near-lossless compression in medical image data [8]. Utilizing wavelet transform and machine learning techniques, it is feasible to classify individuals into categories of colon cancer patients and healthy subjects based on signal analysis. [9]. The method accurately classifies colon cancer patients, providing a robust methodology for distinguishing between health conditions.

Efficient and cost-effective utilization of digital medical imaging in applications like teleradiology and Picture Archiving and Communication Systems (PACS) necessitates advanced image compression techniques. In a comparative study between JPEG and Wavelet compression, the Wavelet Compression Engine and JPEG Wizard tools were employed to compress and decompress a digitized chest X-ray image at various ratios. Wavelet

compression demonstrated lower error matrices and higher peak signal-to-noise ratios, with no significant differences in diagnostic accuracy up to 30:1 compression ratios. Visual comparisons confirmed minimal image degradation, and the wavelet algorithm achieved an impressive compression ratio of up to 600:1. [10]. The Wavelet-Based Deep Auto Encoder-Decoder Network (WDAED) for image compression addresses various frequency components in images. The proposed approach incorporates Wavelet transform pre-processing and a deep super-resolution network in the decoder for improved decompression quality. The algorithm is tested on various datasets, demonstrating superior compression performance across multiple evaluation metrics. [11]. An enhanced algorithm for image compression based on wavelet properties, specifically targeting detail subbands (Diagonal, Vertical, and Horizontal), is analyzed by hard thresholding. Using the standard deviation concept, the proposed algorithm estimates an optimal threshold value for each detail subband. The experiment results demonstrate the algorithm's effectiveness in removing unnecessary wavelet coefficients without compromising image quality. This leads to increased compression ratios and reduced elapsed time, showcasing the potential of the proposed approach. A novel method for enhancing image contrast, termed low dynamic range histogram equalization (LDR-HE), is introduced. This method relies on the Quantized Discrete Haar Wavelet Transform (HWT) in the frequency domain [12].

Investigations are conducted using a hybrid transform for lossless image compression, combining the discrete wavelet transform (DWT) with prediction. The approach involves reversible denoising and lifting steps (RDLSs) with step skipping, applied in an image-adaptive manner using heuristics and entropy estimation. The research demonstrates the effectiveness of combining DWT with prediction, achieving notable compression ratio improvements over JPEG 2000. The study presents practical compression schemes with various trade-offs, providing valuable insights for optimizing compression methods. [13]. Exploring the use of 2-D multiple-level discrete Wavelet transform for image compression shows that after obtaining approximation and detail coefficients through multiple-level Wavelet transform, the superior compression performance of wavelet-based methods compared to other compression techniques was achieved. [14].

Transform coding, especially the Discrete Wavelet Transform (DWT), stands out among effective lossy compression methods. Wavelet-based image coding schemes, including transformation, quantization, and coding, delve into the principles of popular schemes like EZW, SPIHT, SPECK, and EBCOT, comparing their advantages and shortcomings. Designing efficient codecs for wavelet image compression, incorporating spline transform and improved coding schemes. [15].

To address the increasing demand for faster encoding and decoding, researchers proposed an image compression algorithm that combines 2D DWT, PCA, and canonical Huffman coding (CHC). The hybrid compression model achieves up to 60% compression while maintaining high visual quality. Their proposed method effectively utilizes storage space in the growing image data usage era. [16].

The application of two-dimensional discrete wavelet transform (2D DWT) in the compression of both video and still images has been explored, employing innovative compression techniques such as PAQ. The outcomes of this investigation demonstrate that these methods are successful and practical in their applicability [2].

The Huffman coding algorithm compresses and decomposes images by incorporating the Discrete Wavelet Transform. The approach decomposes the image into distinct sets of signals encoded into a bit stream, resulting in improved compression. The proposed algorithm surpasses other techniques in compression ratio, compression time, and bits per pixel. [17].

The critical challenge of signal identification under uncertainty, focusing on filtering and compression using the Discrete Wavelet Transform (DWT), was analyzed in a separate study. The method involved a comparison of the proximity of a one-dimensional series of wavelet coefficients, providing a robust solution. The results underscored wavelets' effectiveness in signal identification and compression, contributing substantially to the existing literature [18].

In another study, innovative image compression techniques are introduced, employing multiwavelets and multiwavelet packets. The research addresses limitations in existing wavelet filters, exploring multiwavelets to provide more design options and combine desirable transform features. Experimental results showcase the superior performance of these techniques, either matching or surpassing current wavelet filters. This research contributes to advancing image compression standards and offers valuable insights for future optimization [19].

A researcher introduces a novel approach to image compression utilizing subspace techniques and downsampling. The methodology begins by reducing the size of the image through downsampling. Subsequently, the Karhunen-Loeve transform (KLT) is employed on the downsampled image to generate a series of transform coefficients [20]. Another study delves into the efficacy of subspace-driven coding methodologies in the context of compression [21]. Another researcher analyzes different Wavelet transforms. The evaluation involves assessing performance using Peak Signal-to-Noise Ratio (PSNR) and Mean Square Error (MSE). The results highlight differences among wavelet families [22].

A researcher evaluated various wavelet difference reduction (WDR) methods, focusing on their image compression and transmission performance. WDR demonstrates coding gains compared to traditional coding approaches, emphasizing the convenience and superiority of modified WDR methods for diverse applications [23].

This study centers around the comprehensive exploration of various wavelet families to evaluate their performance in the domain of image compression.

2. Wavelet Transform

Wavelet transform is a versatile mathematical tool for analyzing signals with dynamic changes in frequency attributes over time. Its applicability extends to signals of one, two, or higher dimensions, preserving unique signal features. This transformative process involves decomposing a signal to obtain a set of basis functions known as wavelets. These wavelets, focused on both frequency and time around specific points, play a pivotal role in achieving approximation through the summation of short-lived waves, aptly named wavelets. The compact support characteristic signifies that wavelets do not extend indefinitely in the signal.

Moreover, wavelets exhibit asymmetry and irregularity, making them valuable in signal processing. The zero-sum area beneath the wavelet curve ensures equal energy distribution in both positive and negative directions. In signal processing, wavelets effectively recover weak signals from noise and analyze signals with dynamic frequency changes over time [22].

$$f = \sum_i a_i \psi_i \tag{1}$$

Choosing scales and positions based on powers of two, known as dyadic scales and positions, enhances the efficiency and accuracy of our analysis. This analytical improvement is achieved through the discrete wavelet transform (DWT), and Mallat developed a particularly efficient implementation of this approach using filters.

The practical filtering algorithm provided by Mallat facilitates a rapid wavelet transform—a process resembling a box through which a signal passes, yielding wavelet coefficients swiftly. This analysis, derived from the discrete wavelet transform (DWT) [14], initiates from the signal s and produces the coefficients $C(a, b)$.

$$C(a, b) = C(j, k) = \sum_{n \in \mathbb{Z}} s(n) g_{j,k}(n) \tag{2}$$

In signal processing, wavelets serve to recover weak signals embedded in noise. Their asymmetric and irregular nature sets them apart. Signal decomposition occurs through scaled and shifted versions of the original Wavelet, termed the mother wavelet, in wavelet analysis. Scaling involves modifying the signal along its time attribute by expanding or compressing it.

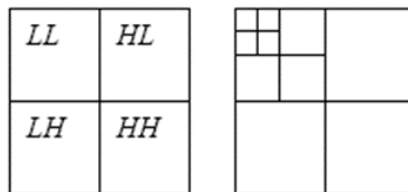


Figure 1. The multilevel decomposition of the image, displaying a 2-level decomposition in this instance

In the process of multilevel image decomposition, the image is systematically broken down into multiple levels or layers to extract detailed information. This intricate procedure involves applying Wavelet transforms that facilitate the isolation of various frequency components within the image. Each level of decomposition reveals specific details, contributing to a more comprehensive understanding of the image's structural and textural characteristics.

Furthermore, this multilevel decomposition allows for extracting both coarse and fine features in the image. The decomposition process operates iteratively, progressively unveiling hidden nuances within the visual data. Through this method, the image's complexity is effectively captured and represented at different scales, providing a hierarchical representation that enhances the analysis of its content.

2.1 Wavelet Families

Different families of wavelets are used in signal processing and analysis. Each wavelet family has its own unique properties and characteristics that make them suitable for various applications. This study investigates the

application of seven well-known wavelet families (haar, dB10, sym7, coif3, bir5.5, rbio2.6, and dmey). These wavelet families are selected based on their widespread recognition and utilization in JPEG 2000. A concise overview of seven widely recognized wavelet families, each distinguished by unique properties and applications in signal processing and image compression.

Haar Wavelet: The Haar wavelet is the most straightforward function operating with two coefficients. It's a piecewise constant function and is computationally efficient. While it lacks smoothness, it's often used in introductory studies due to its simplicity.

dB10 Wavelet: The "dB" in "dB10" stands for Daubechies, a famous family of wavelets known for its compact support and orthogonality. dB10 is a specific wavelet from the Daubechies family, characterized by 10 vanishing moments, which means it captures more complex signal features.

Sym7 Wavelet: This belongs to the Symlets family, an extension of Daubechies wavelets with slightly improved symmetry. Symlets offer good performance in compressing signals with edges and details.

Coif3 Wavelet: Coiflets, or Coiflet wavelets, are similar to Daubechies and Symlets but have a different shape. Coif3, in particular, is from this family and helps analyze signals with finite support.

Bior5.5 Wavelet: Bior stands for "Biorthogonal" wavelets, which use separate sets of functions for decomposition and reconstruction. The 5.5 represents the number of vanishing moments in each of these functions. Biorthogonal wavelets like Bior5.5 are valuable for handling non-stationary signals.

Rbio2.6 Wavelet: Another member of the biorthogonal wavelet family, Rbio2.6, has different characteristics compared to Bior5.5. The numbers in the name indicate the number of vanishing moments for the analysis and synthesis wavelets, respectively.

Dmey Wavelet: The Dmey wavelet, also known as the Meyer wavelet, is derived from a function introduced by Yves Meyer. It's characterized by smoothness and symmetry and is often used in image compression and denoising applications.

Each of these wavelets has specific properties regarding frequency response, vanishing moments, support, and other characteristics that make them suitable for different types of signal analysis, compression, and feature extraction tasks. The choice of Wavelet depends on the specific requirements and characteristics of the signal being analyzed or processed.

3. Method: Wavelet-Based Image Compression and Reconstruction

Image compression using wavelets involves transforming and analyzing individual images. Wavelet transforms and decomposes an image into its frequency components, creating a multi-resolution representation. This transformation allows for efficient compression by removing redundant or less noticeable image data while preserving crucial visual information. Figure 2 illustrates the sequential steps involved in image processing, commencing with the application of wavelet transform, followed by quantization, coding, and culminating in the generation of the compressed image.

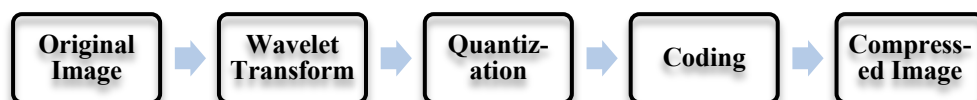


Figure 2. The block diagram illustrates the image compression process employing Wavelet transform.

Wavelet-based image compression typically involves spatial information compression. It takes advantage of the spatial redundancy present in images, identifying and reducing unnecessary pixel data while retaining essential details.

In multilevel wavelet decomposition, images are divided into sub-bands like LL (low-low), LH (low-high), HL (high-low), and HH (high-high) using the wavelet transform. These sub-bands represent different frequency components of the image.

This compression technique finds applications in various fields, such as photography, medical imaging, satellite imagery, and digital libraries, where single images must be stored, transmitted, or processed efficiently.

Upon transforming image data through wavelets, the subsequent application of thresholding and quantization processes becomes imperative. Subband thresholding is a technique used in signal processing and image compression. It involves dividing a signal or image into different frequency bands or subbands and applying a threshold to the coefficients within these subbands. This thresholding helps to reduce less significant or noisy information, leading to compression [24].

Quantization, as a crucial step in the image compression workflow, reduces the number of symbols within the data matrix. This process is essential for efficiently compressing data and optimizing memory usage. The wavelet coefficients undergo quantization using a carefully selected quantizer, ensuring that the transformed data is represented with an appropriate level of precision while effectively managing storage requirements. The meticulous application of quantization aligns with the overarching goal of image compression, enabling the preservation of essential information while minimizing the memory footprint of the compressed data.

Following the quantization process, the data undergo compression, particularly in image compression, where quantization and coding techniques are employed. In image compression workflows, lossy compression techniques are expected to be used at this stage. The outcome of this process is the acquisition of compressed images characterized by a significantly reduced file size. This reduction in file size is a key objective in image compression, allowing for more efficient storage, transmission, and handling of visual data while acknowledging the inherent trade-offs associated with lossy compression methods.

Huffman coding is a widely used entropy coding algorithm in information theory and compression. A variable-length coding method assigns shorter codes to more frequent symbols and longer codes to less frequent symbols. Huffman coding is often used to compress data efficiently, and it's a key component in many compression algorithms.

Huffman coding stands as a widely adopted algorithm for achieving image compression. This algorithm meticulously analyzes the frequencies of pixel values, assigning shorter codes to frequently occurring symbols and longer codes to those that are less common, resulting in the construction of a Huffman tree. However, the conventional Huffman coding approach necessitates the decoder to traverse the entire tree, introducing potential inconvenience. The classical Huffman algorithm has been extensively employed in both data compression and image compression applications. One notable drawback of the traditional Huffman algorithm is its reliance on variable-length codes for symbol representation dictated by their frequency of occurrence. Although this strategy effectively compresses frequently encountered symbols, it may generate lengthier codes for symbols that occur less frequently.



Figure 3. Block diagram for the reconstruction of the compressed image.

Following the acquisition of the compressed image, the processes mentioned above are reversed, as illustrated in the block diagram presented in Figure 3. The decoding process involves reversing compression, wherein the compressed image undergoes dequantization. Subsequently, an inverse wavelet transform is applied to restore the original data structure. The culmination of these processes leads to reconstructing the image in its original form. This intricate series of operations ensures that the information lost during compression is recuperated, restoring the visual data to its pre-compressed state.

3.1. Development of the Novel NWI Wavelet in Image Compression

In this research, a novel wavelet is developed and explicitly proposed for image compression, referred to as "new wavelet for image compression" or NWI. This new Wavelet is a variant of the Daubechies filter, with enhanced performance observed when scaling function frequency and vanishing moment are increased [24]. Well-localized elements characterize the NWI wavelet family. A set of N integer coefficients defines each Wavelet in the family represented as $k = \{0, 1, \dots, N - 1\}$, established through scale relations in Equation 3 and 4. The coefficients a_k and a_{1-k} , featured in Equations 3 and 4, are filter coefficients, and their relationships are expressed [25] as;

$$\phi(x) = \sum_{k=0}^{N-1} a_k \phi(2x - k) \quad (3)$$

$$\psi(x) = \sum_{k=2-N}^1 (-1)^k a_{1-k} \phi(2x - k) \quad (4)$$

Figure 4.a) displays the proposed wavelet family, NWI 20, while Figure 4.b) illustrates the mother wavelet, Daubechies 10. These figures provide visual representations of the wavelet functions, highlighting the distinctive characteristics of the newly introduced NWI 20 wavelet and comparing it to the well-established Daubechies 10 wavelet.

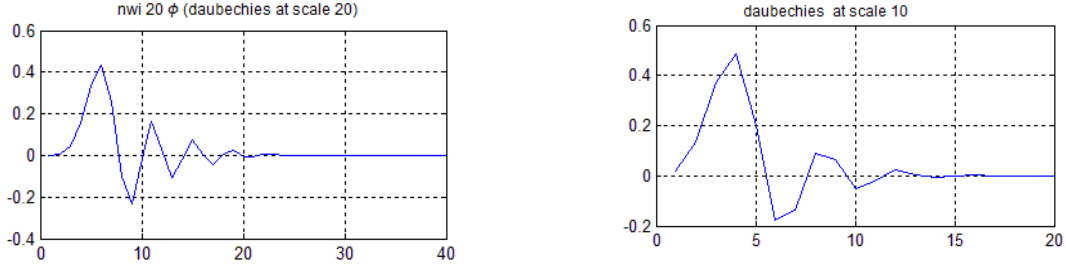


Figure 4. a) NWI wavelet b) daubechies wavelet

Standard test images such as Lena, house, lake, and tree are chosen to assess the efficacy of these wavelet transformations. These images are widely recognized and serve as benchmarks for readers' convenience in image compression.

3.2 Measurement of Image Quality

In lossy compression, the reconstructed image's pixel values differ from the original image's pixel values. If the difference between the original and reconstructed images is imperceptible to the human eye, it signifies good compression. In this study, the Peak signal-to-noise ratio (PSNR) has been used to measure the quality of the reconstructed image. The PSNR serves as a metric to quantify the peak error in decibels. Its relevance is constrained to data encoded in terms of bits per sample or bits per pixel. A higher PSNR value corresponds to enhanced quality in the compressed or reconstructed image. In the context of lossy compression, typical PSNR values for an image range between 30 and 50 dB. Notably, the two images become indistinguishable when the PSNR surpasses 40 dB. The following equation defines the PSNR:

$$PSNR = 10 \log_{10} \left(\frac{\max^2}{MSE} \right) \quad (5)$$

max: color depth. For 8 bits $\max=2^8-1=255$, and mean square error can be calculated with Equation 6;

$$MSE = \frac{1}{mn} \sum_{i=0}^{m-1} \sum_{j=0}^{n-1} |X(i, j) - X_c(i, j)|^2 \quad (6)$$

Where, M and N represents the size of the image, X represents the given input image and X_c represents the reconstructed image.

The compression ratio (CR) is defined as the proportion of elements in the compressed image to the number of elements in the original image, expressed as a percentage. It is employed to determine the compression percentage attained by a compression algorithm, calculated through the Equation 7.

$$CR = \left(1 - \frac{h_c}{h_i} \right) * 100 \quad (7)$$

Where h_c : number of bits of the compressed image, h_i : number of bits of the initial image

The Compression Performance (CP) metric, initially introduced by Bulut et al. [26], combines the Peak Signal-to-Noise Ratio (PSNR) as the quality measure and Compression Ratio (CR) as the compression metric. This hybrid metric effectively captures the correlation between PSNR and CR, enabling a comprehensive assessment of compression performance. The formulation of CP in Equation 8 as follow;

$$CP = PSNR \times CR \quad (8)$$

A higher CP value indicates superior performance in image compression, emphasizing the ability to achieve higher levels of compression without compromising image quality.

All selected test images undergo compression using the seven established wavelet families and the newly developed NWI wavelet. The results are then evaluated using two key performance metrics: Compression Ratio (CR), Peak signal-to-noise ratio (PSNR) and Compression Performance (CP). This comprehensive analysis aims to provide insights into the comparative performance of different wavelet families, including the innovative NWI wavelet, in the context of image compression.

4. Results and Discussions

This study systematically evaluates the performance of eight distinct wavelet families, including the proposed "NWI" wavelet, using eight diverse test images, consistently employing the Huffman compression method across all wavelet families. The uniform use of Huffman compression allows for an analysis of the efficacy of the wavelet families while minimizing the impact of coding variations in the process [27]. The objective is to evaluate the overall effectiveness of these wavelet families and compare them with the developed and proposed NWI Wavelet across a spectrum of images, aiming to gain a comprehensive understanding of their performance variations in diverse scenarios.

In this study, we utilized a set of standard, widely recognized test images for our analysis as shown in Figure 5. The images chosen include House, Lenna, Lake, and Tree, which were specifically selected to assess medium to low-frequency responses of the wavelet families. Additionally, Peppers, Baboon, Boat, and Airplane images were incorporated to evaluate the high-frequency response of the wavelet families.

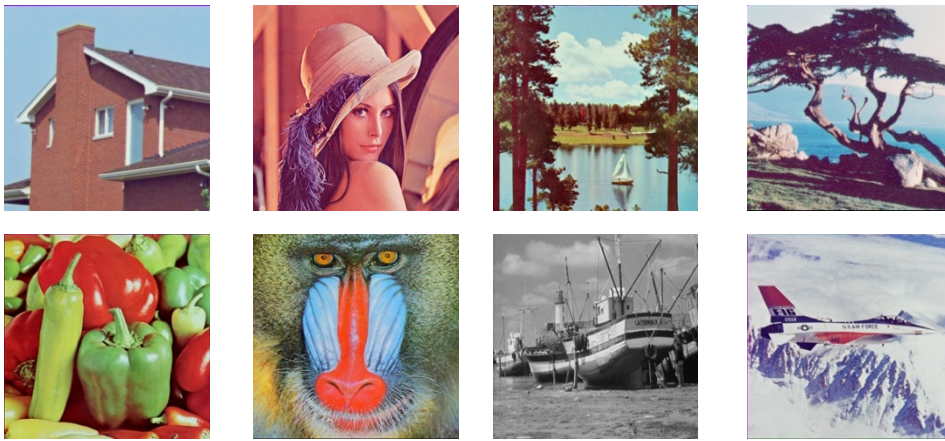


Figure 5. Eight test images, arranged from top left to right as House, Lenna, Lake, Tree, and from bottom left to right as Peppers, Baboon, Boat, and Airplane.

Figure 6 offers an exhaustive examination of the compression performances demonstrated by eight distinct wavelet families across eight test images. The analysis encompasses a range of threshold values applied with Huffman coding, allowing for exploring diverse compression ratios. This comprehensive evaluation provides valuable insights into the varying capabilities of each wavelet family in achieving optimal compression results for the specified test images under different threshold settings, thereby contributing to a nuanced understanding of their performance characteristics. The results depicted in Figure 6.a) and 6.b) highlight notable similarities in the compression outcomes for the House and Lenna images, wherein the difference in image quality between the best and worst-performing wavelet family is approximately 3 dB. Sym7 and Coif3 emerge as the top-performing wavelet families, while rbio2.6 exhibits the least favorable performance. Considering the proposed NWI wavelet, it exhibits superior performance compared to the other seven wavelet families.

The reconstructed image quality is approximately 1 dB higher than that achieved with the Coif3 wavelet. This enhancement in performance highlights the efficacy of the proposed NWI wavelet in image reconstruction, demonstrating its potential for superior results compared to established wavelet families.

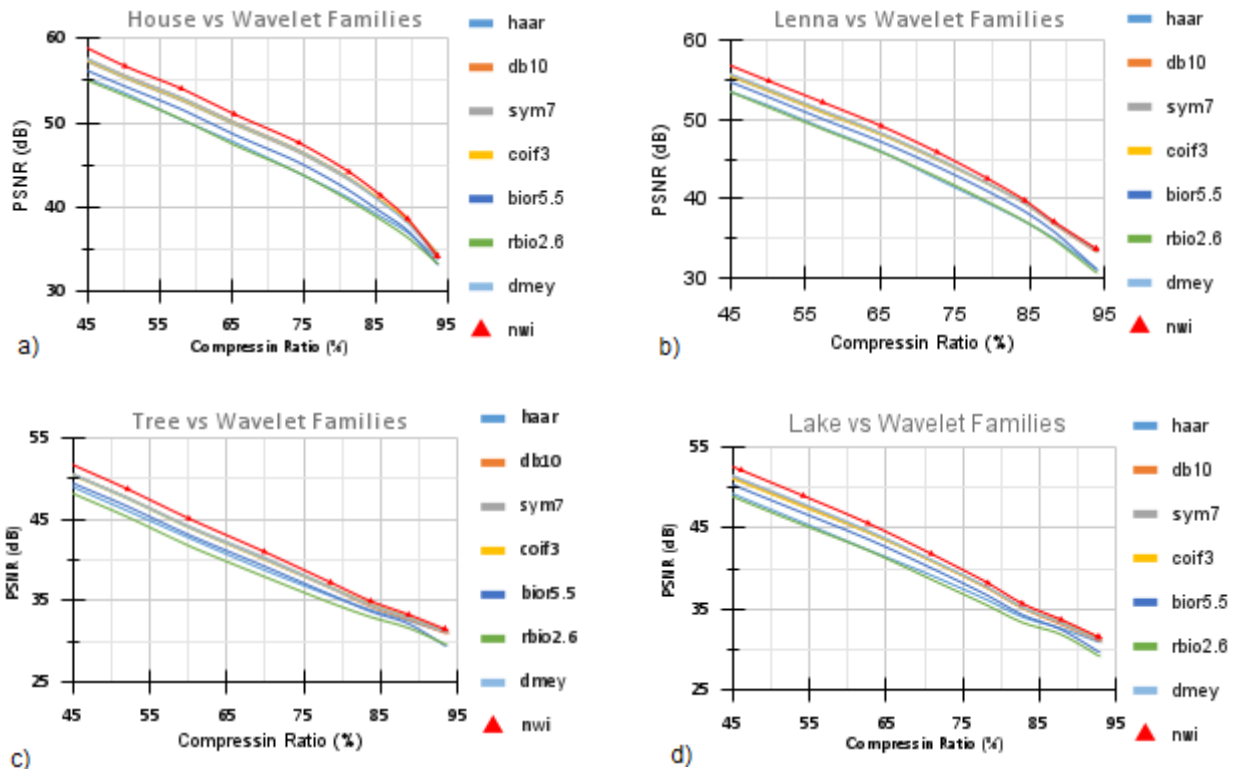


Figure 6. Comparison of Peak Signal-to-Noise Ratio (PSNR) against Compression Ratio (CR) for Eight Wavelet Families across Four Test Images.

In the case of Lake and Tree images, a consistent trend is observed, with their image quality registering approximately 5 dB lower for all wavelet families compared to the House and Lenna images, as depicted in Figure 6.c) and Figure 6.d). Sym7 and coif3 consistently deliver optimal performance, while rbio2.6 consistently yields the least favorable results. It is crucial to emphasize that the x-axis of the figure illustrates the compression ratio, ranging between 45% and 95%.

Likewise, the proposed NWI wavelet demonstrates enhanced compression performance for the tree and lake datasets. It yields results that are 1 dB superior compared to Sym7 and Coif3 wavelets. This improvement underscores the effectiveness of the proposed NWI wavelet in achieving higher compression efficiency, displaying its potential advantages over established wavelets like sym7 and coif3.

Figure 7 depicts the performance assessment of various wavelet families applied to four additional test images: Peppers, Baboon, Boat, and Airplane. Each graph within the figure represents the performance of a specific wavelet family in terms of compression ratio (CR) versus peak signal-to-noise ratio (PSNR) for each test images. This comprehensive evaluation offers valuable insights into the diverse capabilities of each wavelet family in achieving optimal compression outcomes for the specified test images across various threshold settings, thus contributing to a nuanced comprehension of their performance characteristics. Notably, the results for the Peppers image, as depicted in Figure 7.a), showcase the best performance among the four additional test images. Conversely, the Baboon image, shown in Figure 7.b), exhibits the lowest performance, registering a notable 8 dB less compared to the average performance. Among the evaluated wavelet families, Sym7 and Coif3 emerge as the top performers, while Rbio2.6 demonstrates the least favorable performance.

Introducing the proposed NWI wavelet it performs better than the other seven wavelet families. The reconstructed image quality with NWI is approximately 1 dB higher than that achieved with the Coif3 wavelet, underscoring its efficacy in image reconstruction and its potential for superior results compared to established wavelet families.

A consistent trend is observed for the Boat and Airplane images, with their image quality depicted in Figure 7.c) and Figure 7.d), respectively. Dmey and Coif3 consistently deliver optimal performance, while Rbio2.6 consistently yields the least favorable results.

Furthermore, the proposed NWI wavelet demonstrates enhanced compression performance across the four image datasets, yielding results that are 1.5 dB superior compared to Sym7 and Coif3 wavelets. This improvement underscores the effectiveness of the proposed NWI wavelet in achieving higher compression efficiency, highlighting its potential advantages over established wavelets such as Sym7 and Coif3.

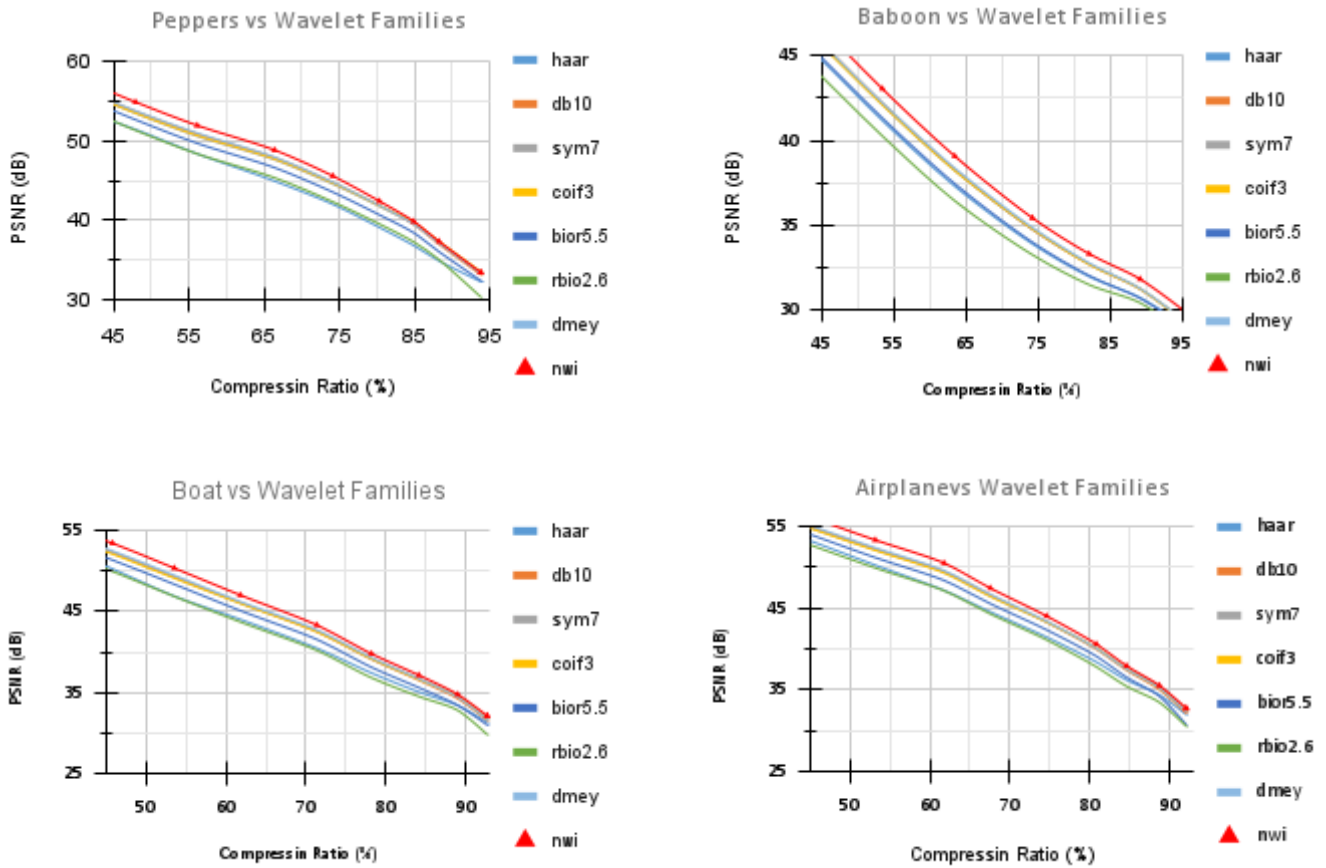


Figure 7. Comparison of Peak Signal-to-Noise Ratio (PSNR) against Compression Ratio (CR) for seven wavelet families across four additional test images..

Figure 8.a) illustrates compressed and reconstructed house images chosen from the test dataset as an exemplar leveraging the NWI wavelet family. The original and reconstructed image disparities, depicted as residuals, reveal that regions colored black signify the attainment of high image quality. This visualization effectively demonstrates the effectiveness of the NWI wavelet family in preserving image quality during the compression and reconstruction processes.

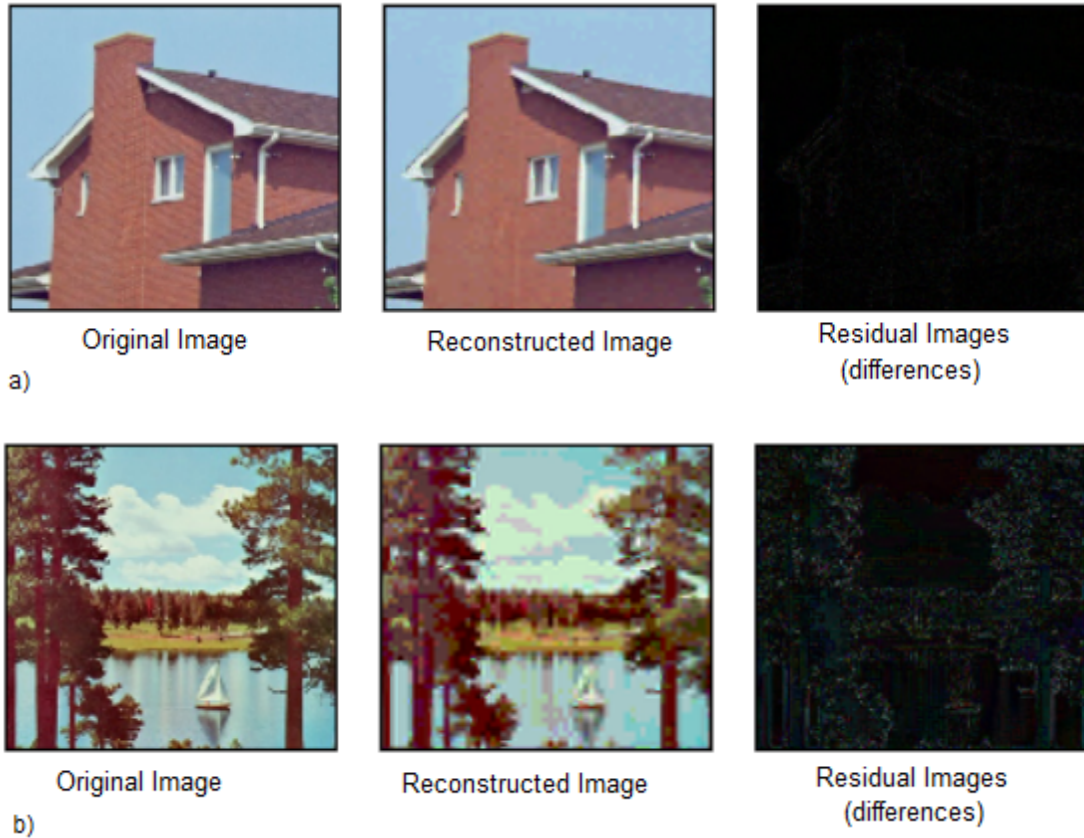


Figure 8. Utilizing the wavelet family "NWI", a) the original versus the compressed and reconstructed Test Image-1, and b) the original versus the compressed and reconstructed Test Image-4.

Figure 8.b) presents another illustrative example from our image dataset. Here, the lake image undergoes compression and reconstruction utilizing the NWI wavelet family, visually representing the process. The residuals, depicting the differences between the original and reconstructed images, exhibit certain image textures. This observation suggests a lower Peak signal-to-noise ratio (PSNR) compared to the house image. The nuanced variations in residual patterns contribute to a comprehensive understanding of the NWI wavelet family's performance across different images.

Table 1 presents a detailed analysis of the compression performances of various wavelet families while maintaining a constant Peak Signal-to-Noise Ratio (PSNR) of 40 dB. The table also includes summary statistics such as average (Avg) and standard deviation (Stdev) PSNR values across all wavelet families for each test image, providing a comprehensive overview of their performance. Notably, Nvi, Coif3, and dB10 demonstrate superior Compression Ratios (CR), achieving values of 76.00%, 75.95%, and 75.55%, respectively. In contrast, Haar and Rbio2.6 exhibit relatively lower CR performances, registering 72.62% and 72.52% values. The highest PSNR value of 41.58 dB is observed in the House image, indicating excellent compression quality, while the lowest PSNR performance of 32.5 dB is noted in the Baboon image.

Examining the standard deviation values in the last row of the table reveals variations in image quality among different wavelet families, ranging from 0.41 to 1.27. This suggests a relatively consistent performance correlation across the families. However, the standard deviation values for the average PSNR range from 7.75 to 10.06, indicating that the images' characteristics influence the performance of wavelet families.

Moreover, Coif3 and Sym7 demonstrate commendable CR values across various test images, indicating superior performance. Conversely, Rbio2.6 and Haar exhibit relatively lower CR performances. The proposed NWI wavelet shows promising CR performance, positioning it as a compelling option for image compression. Its consistent performance and good CR make it a valuable addition to existing wavelet families, potentially offering enhanced versatility in various compression scenarios.

The performance of the NWI wavelet, achieving 76% in our study, is particularly noteworthy, demonstrating superior CR values across a set of test images. This observation underscores the NWI wavelet's potential as a

valuable option for efficient image compression, competing favorably with established wavelet families like Coif3 and Sym7.

Table 1. Performance of Test Images at a Constant PSNR of 40 dB with Compression Ratio (CR).

Wave Family	Lenna	House	Lake	Tree	Peppers	Baboon	Boat	Airplane	Avg	Stdev
haar	78.36	83.28	69.41	67.78	79.36	51.2	72.34	77.6	72.42	10.06
db10	80.83	84.16	71.08	69.86	83.03	56.96	72.66	77.78	74.55	8.95
sym7	81.80	85.69	71.87	70.37	81.8	58.48	73.01	78.68	75.21	8.69
coif3	82.62	85.89	72.07	71.28	83.47	58.52	74.68	79.06	75.95	8.88
bior5.5	81.29	83.98	71.15	70.81	81.29	59.47	74.88	78.16	75.13	7.96
rbio2.6	80.08	82.47	67.86	66.00	81.06	55.1	71.2	77.22	72.62	9.42
dmey	81.54	84.05	71.47	70.96	82.13	56.03	72.29	78.74	74.65	9.14
NWI20	83.08	85.77	70.36	73.79	81.31	61.59	74.92	77.17	76.00	7.75
Avg	81.20	84.41	70.66	70.11	81.68	57.17	73.25	78.05	72.54	10.81
Stdev	1.49	1.26	1.41	2.35	1.19	2.95	1.32	0.67	1.53	0.99

Table 2 thoroughly examines the Peak Signal-to-Noise Ratio (PSNR) image quality achieved under a consistent 80% compression ratio, shedding light on the efficacy of various wavelet families applied to the test images. The inclusion of statistical metrics in the last two columns of the table further enriches the analysis by providing insights into the average and standard deviation for each wavelet family.

Significant performance disparities emerge among the wavelet families, with Nvi, Dmey, and Coif3 emerging as the top performers, boasting PSNR values of 39.10, 38.52, and 38.07 dB, respectively. Conversely, Haar and Rbio2.6 exhibit comparatively inferior PSNR performance, clocking in at 36.99 and 37.68 dB values. The disparity in PSNR values underscores the varying effectiveness of different wavelet families in preserving image quality under compression.

Table 2. Performance of Test Images at a Constant Compression Ratio of 80% with Peak Signal-to-Noise Ratio (PSNR) Values.

Wave Family	PSNR (dB) image quality									AVG	Stdev
	Lenna	House	Lake	Tree	Peppers	Baboon	Boat	Airplane			
haar	39.18	41.64	35.32	34.96	39.02	30.42	36.43	38.93	36.99	3.48	
db10	40.46	41.63	35.54	34.93	41.46	31.69	37.54	38.69	37.74	3.52	
sym7	41.45	42.42	35.93	35.18	41.05	31.72	38.02	38.75	38.07	3.64	
coif3	41.86	42.48	36.04	35.64	40.85	33.78	38.64	35.64	38.12	3.30	
bior5.5	40.98	41.08	35.58	35.4	40.21	32.52	39.13	39.22	38.02	3.13	
rbio2.6	39.68	40.21	34.82	34.45	41.55	32.63	38.24	39.82	37.68	3.26	
dmey	41.6	41.62	35.73	35.48	41.63	33.76	38.72	39.59	38.52	3.15	
NWI20	41.54	42.89	37.25	36.90	41.98	33.48	38.96	39.82	39.10	3.14	
Avg	40.84	41.58	35.57	35.15	40.97	32.50	38.21	38.81	37.62	3.61	
Stdev	0.98	0.78	0.41	0.41	0.90	1.11	0.83	1.27	1.03	0.20	

Highlighting individual image performance, the House image stands out with the highest average PSNR value of 41.58 dB, indicative of superior compression quality. On the contrary, the Baboon image demonstrates the lowest PSNR performance at 32.5 dB, signaling challenges in preserving image fidelity for certain content types.

A closer examination of the standard deviation values in the table's last row reveals the range of variation in image quality among different wavelet families, spanning from 0.41 to 1.27. This suggests a relatively consistent performance correlation across the families, indicating their overall reliability in maintaining image quality. However, the standard deviation values for the average PSNR paint a nuanced picture, ranging from 3.13 to 3.64.

This indicates that while wavelet families exhibit consistent performance trends, their effectiveness is indeed influenced by the inherent characteristics of the images themselves, underscoring the complexity of image compression dynamics.

Furthermore, the proposed NWI20 consistently delivers superior results across various image types, underscoring its efficacy in image compression. This observation aligns with our expectations, highlighting the advantageous performance of the proposed NWI wavelet. It's essential to note that the type of image significantly influences the attained image quality, emphasizing the need for tailored compression strategies based on image content.

Table 3 presents detailed information on the average Compression Ratio (CR) and Peak Signal-to-Noise Ratio (PSNR) achieved across ten compression levels for all test images. Notably, Coif3 and Sym7 demonstrate commendable CR, indicating superior performance across various test images. Conversely, Rbio2.6 and Haar exhibit relatively lower CR. The newly introduced NWI Wavelet shows promise with its CR performance. Overall, the trend highlights NWI and Coif3 as favorable choices for image compression due to their high average PSNR values and consistent performance. Low standard deviation values suggest minimal performance variations among wavelet families, indicating comparable effectiveness in diverse compression scenarios. The performance of the NWI wavelet is particularly noteworthy, demonstrating superior CR across diverse test images and showcasing competitive results compared to established wavelet families like Coif3 and Sym7. Its consistent performance and good CR make it a compelling option for applications requiring efficient image compression, potentially offering enhanced versatility in various compression scenarios.

Table 3. Average Compression Ratio (CR) and average Peak Signal-to-Noise Ratio (PSNR) achieved for the test images at 10 compression levels, utilizing various wavelet families.

		haar		db10		sym7		coif3		bior5.5		rbio2.6		dmey		NWI20	
		CR	PSNR	CR	PSNR	CR	PSNR	CR	PSNR	CR	PSNR	CR	PSNR	CR	PSNR	CR	PSNR
Lenna	Avg	72.79	41.74	71.45	43.94	72.19	43.88	72.59	43.96	74.17	42.72	74.03	41.64	72.07	44.03	72.78	44.66
	Stdev	18.28	8.28	17.41	8.31	17.54	8.15	17.29	8.14	17.82	8.65	17.79	8.38	17.59	8.26	18.78	8.63
House	Avg	73.36	43.62	69.90	45.44	71.42	45.37	71.49	45.47	72.68	44.20	72.77	43.33	70.62	45.43	71.69	46.20
	Stdev	20.12	8.76	20.33	9.36	20.54	9.09	20.32	9.16	20.54	9.35	20.51	8.95	20.52	9.33	21.75	9.76
Lake	Avg	70.65	39.25	68.46	40.63	69.04	40.64	69.47	40.62	70.69	39.63	71.24	38.54	68.27	40.75	70.95	41.44
	Stdev	19.55	7.60	21.12	8.36	21.04	8.18	20.55	8.15	20.75	8.40	21.03	8.03	21.30	8.34	22.07	8.66
Tree	Avg	70.17	39.37	68.11	40.22	68.81	40.38	69.71	40.26	70.64	39.22	70.63	38.40	68.95	40.28	70.37	41.06
	Stdev	20.58	7.82	21.85	8.43	21.29	8.34	20.99	8.28	21.24	8.46	21.24	7.99	21.54	8.34	22.81	8.73
Peppers	Avg	72.59	41.62	71.26	43.85	72.34	43.82	72.21	43.90	73.18	42.82	73.77	41.44	71.42	43.96	69.59	44.56
	Stdev	19.19	7.82	19.24	8.30	19.24	8.08	18.52	8.06	18.68	8.19	19.40	8.37	19.15	8.27	20.01	8.67
Baboon	Avg	66.33	37.75	66.06	38.54	66.55	38.51	66.74	38.49	66.66	37.86	67.00	37.10	66.69	38.60	66.08	39.33
	Stdev	24.88	8.96	24.64	9.45	24.55	9.38	24.50	9.37	24.39	9.29	24.79	9.09	24.69	9.47	24.84	9.71
Boat	Avg	70.64	40.39	68.76	41.85	69.64	41.90	70.10	41.85	70.98	40.99	71.68	39.75	68.98	42.00	67.98	42.64
	Stdev	20.09	7.99	20.64	8.58	19.88	8.45	19.83	8.41	20.08	8.47	20.64	8.32	20.39	8.56	21.52	8.83
Airplane	Avg	74.04	40.96	71.95	42.33	72.38	42.37	72.77	42.36	74.49	41.28	74.68	40.30	72.09	42.48	70.95	43.10
	Stdev	16.62	7.60	17.52	8.27	16.95	8.11	16.91	8.07	17.54	8.34	17.50	7.98	17.53	8.23	18.65	8.50

The standard deviation (Stdev) values reflect the consistency of the proposed method's performance, showing relatively lower variations. These results underscore the robustness and superior performance of the proposed NWI wavelet across various compression scenarios. However, choosing the best wavelet family may also depend on specific application requirements.

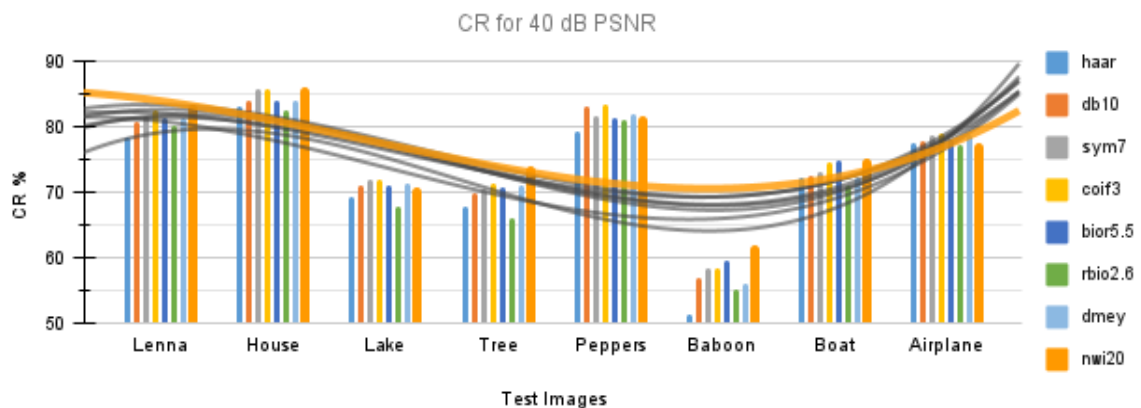
The compression performance of various wavelet families was assessed using Compression Performance (CP) values across a range of test images. Table 4 provides an overview of the Compression Performance (CP) exhibited by various wavelet families across different test images. The highest CP value observed is 3312.08, achieved by the NWI20 wavelet in the House image, which represents the proposed method. Conversely, the lowest CP value of 2485.80 is obtained with the rbio2.6 wavelet in the Baboon image.

Table 4. Compression Performance of test images, utilizing various wavelet families

	Compression Performance (CP)							
	haar	db10	sym7	coif3	bior5.5	rbio2.6	dmey	NWI20
Lenna	3038.25	3139.51	3167.70	3191.06	3168.54	3082.61	3173.24	3250.35
House	3199.96	3176.26	3240.33	3250.65	3212.46	3153.12	3208.27	3312.08
Lake	2773.01	2781.53	2805.79	2821.87	2801.44	2745.59	2782.00	2940.17
Tree	2762.59	2739.38	2778.55	2806.52	2770.50	2712.19	2777.31	2889.39
Peppers	3021.22	3125.05	3169.55	3170.12	3133.45	3057.07	3139.22	3100.80
Baboon	2504.14	2545.93	2562.75	2568.50	2523.87	2485.80	2573.96	2598.72
Baot	2853.41	2877.21	2917.75	2933.17	2908.91	2849.44	2897.32	2898.48
Airplane	3033.11	3045.38	3066.97	3082.73	3075.18	3009.88	3062.66	3057.84

Notably, NWI20 and Coif3 consistently demonstrated superior compression performance, with NWI20 exhibiting particularly high CP values, notably in the House image. Sym7 also showcased commendable compression performance across diverse test images. However, DB10 and Dmey displayed moderate performance, with CP values generally falling within a moderate range. In contrast, Haar, rbio2.6, and bior5.5 exhibited relatively lower compression performance, with CP values tending to be on the lower end of the spectrum across most test images.

Figures 9 illustrate the trend lines depicting the relationship between wavelet families and their corresponding performances in both PSNR and CR. In Figure 9, the compression ratios of eight selected wavelet families are depicted for images with a quality of 40 dB. The graph illustrates the variations in compression ratios among the wavelet families, with a discernible trend line capturing these differences. Notably, the house image attains the highest compression ratio, signifying superior compression efficiency compared to the other test images. Conversely, the Baboon image exhibits the lowest compression ratio, indicating less optimal performance in achieving data reduction. This graphical representation offers a clear visual insight into how the selected wavelet families perform regarding compression ratios at a specific image quality level.

**Figure 9.** Compression performance of wavelet families for test images.

In Figure 10, the image quality, as measured by PSNR values, is presented at a fixed compression ratio of 80%. The graph highlights the performance of various test images across this compression level. Impressively, the house image stands out with the highest quality, indicating its resilience to compression at the specified ratio. Additionally, the PSNR values for the Peppers test image closely approach those of the house image, emphasizing their comparable high-quality retention. On the other hand, the Lake and Baboon test images exhibit PSNR values approximately 8 dB lower than those of the House and Peppers. This detailed analysis provides valuable insights into the varying image qualities achieved by the tested compression methods under the defined conditions.

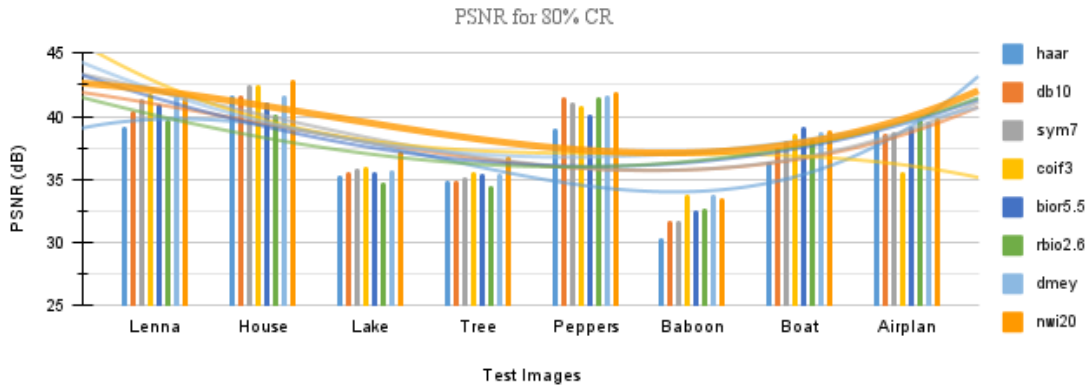


Figure 10. PSNR values of test images for fixed 80%compression ratio for different wavelet families.

The table and figure information suggests a connection between image specifications, specifically entropy, and the impact of different wavelet families on compression ratio and image quality. The observed results indicate that the choice of wavelet family significantly influences the performance. Notably, Coif3, characterized by a high-frequency converter, demonstrates superior compression ratio and image quality performance compared to other wavelet families. This emphasizes the importance of selecting an appropriate wavelet family based on specific image characteristics and compression requirements.

By assessing and comparing performance metrics, specifically Compression Ratio (CR) and Peak signal-to-noise Ratio (PSNR), one can effectively determine an appropriate wavelet transform for a specific image processing application. The CR and PSNR values analysis proves instrumental in selecting the optimal Wavelet for a given task. Notably, PSNR values ranging from 30 to 40 dB are generally deemed satisfactory across various applications. However, it is imperative to validate the suitability of wavelets individually for each application, ensuring an optimal match between the chosen Wavelet transform and the specific requirements of the image processing task at hand.

5. Conclusions

In conclusion, the comprehensive evaluation of various wavelet families for image compression performance, as detailed in the tables and figures, provides in-depth insights into their respective influences on compression ratio and image quality. The results emphasize the crucial role of selecting an appropriate wavelet family tailored to specific image characteristics and desired compression goals. Notably, Coif3, distinguished by its high-frequency conversion capabilities, is a standout performer, showcasing superior results across the assessed parameters.

Additionally, including the proposed NWI wavelet in the evaluation further enhances the understanding of its performance characteristics. The NWI wavelet consistently exhibits competitive results, demonstrating its potential as a viable option in image compression scenarios. These findings significantly contribute to the broader comprehension of wavelet-based image compression, offering practical guidance for optimizing performance across diverse applications.

As the field of image compression continues to advance, ongoing investigations and refinements in wavelet selection and compression techniques are essential to fuel continued progress in image processing. Integrating innovative wavelets, such as the NWI wavelet, into the existing landscape further expands the possibilities for achieving enhanced compression outcomes and improved image quality.

References

- [1] Ayiluri SR, Yelchuri SK, Laxumudu V, Sajan GP, Kumar, AYP, Kaur K. Jpeg Image Compression Using Matlab. International Research Journal of Modernization in Engineering Technology and Science. 2022;3(5) :663-669
- [2] Oz I. İki boyutlu ayrık dalgacık dönüşüm filtreleri kullanarak sabit ve hareketli görüntü sıkıştırma. PhD, Sakarya University, Sakarya, Turkey, 2006.
- [3] Aranzado, J. D. R., Barbosa, G. K., Linget, K. F., & Agustin, V. A. Enhancement of the Huffman Algorithm with Discrete Wavelet Transform Applied to Lossless Image Compression.
- [4] Bulut, F. Low dynamic range histogram equalization (LDR-HE) via quantized Haar wavelet transform. The Visual Computer, 2022;38(6), pp.2239-2255

- [5] Chen Y. An introduction to wavelet analysis with applications to image and jpeg 2000. In 2022 4th International Conference on Intelligent Medicine and Image Processing. 2022; pp. 49-57.
- [6] Wang D, Zhang L, Vincent, A. Improvement of JPEG2000 using curved wavelet transform. In Proceedings.(ICASSP'05). IEEE International Conference on Acoustics, Speech, and Signal Processing, 2005; Vol. 2, pp. ii-365, IEEE.
- [7] Yilmaz Ö, Aksoy M, Kesilmiş Z. Misalignment fault detection by wavelet analysis of vibration signals. International Advanced Researches and Engineering Journal, 2019; 3(3), 156-163.
- [8] Viswanthan P, Kalavathi P. Subband Thresholding for Near-Lossless Medical Image Compression. International Journal of Computing and Digital Systems. 2023;14(1), 1-1.
- [9] Toraman S, Turkoglu I. A new method for classifying colon cancer patients and healthy people from FTIR signals using Wavelet transform and machine learning techniques. Journal of the Faculty of Engineering and Architecture of Gazi University. 2020; 35(2), 933-942.
- [10] Saffor A, Ramli AR, Ng KHA. Comparative study of image compression between JPEG and Wavelet. Malaysian Journal of computer science. 2001;14(1), 39-45.
- [11] Mishra D, Singh SK, Singh RK. Wavelet-based deep auto encoder-decoder (wdaed)-based image compression. IEEE Transactions on Circuits and Systems for Video Technology. 2020; 31(4), 1452-1462.
- [12] Taujuddin NSAM, Ibrahim R, Sari S. An improved technique to wavelet thresholding at details subbands for image compression. ARPN Journal of Engineering and Applied Sciences. 2016;11(18), 10721-10726.
- [13] Starosolski R. Hybrid adaptive lossless image compression based on discrete wavelet transform. Entropy. 2020; 22(7), 751.
- [14] Oz I, Oz C, Yumusak N. Image compression using 2-D multiple-level discrete wavelet transform (DWT). Eleco 2001 International Conference on Electrical and Electronics Engineering 2001; Turkey.
- [15] Boujelbene R, Jemaa YB, Zribi M. A comparative study of recent improvements in wavelet-based image coding schemes. Multimedia Tools and Applications. 2019; 78, 1649-1683.
- [16] Ranjan R, Kumar P. An Improved Image Compression Algorithm Using 2D DWT and PCA with Canonical Huffman Encoding. Entropy.2023; 25(10), 1382.
- [17] Aranzado JDR, Barbosa GK, Linget KF, Agustin VA. Enhancement of the huffman algorithm with discrete wavelet transform applied to lossless image compression. United International Journal for Research & Technology. 2023; Volume 04, Issue 08, pp 83-90.
- [18] Onufriienko D, Taranenko Y. Filtering and compression of signals by the method of discrete wavelet decomposition into one-dimensional series. Cybernetics and Systems Analysis. 2023;1-8.
- [19] Martin MB, Bell AE. New Image compression techniques using multiwavelets and multiwavelet packets. in IEEE Transactions on Image Processing, 2001; vol. 10, no. 4, pp. 500-510.
- [20] Keser S. An image compression method based on subspace and down sampling. Bitlis Eren Üniversitesi Fen Bilimleri Dergisi, . 2023;12(1), 215-225
- [21] Keser S, Gerek ÖN, Seke E, Gülmezoğlu MBA. Subspace based progressive coding method for speech compression. Speech Communication, ,2017; 94, 50-61.
- [22] Bindulal TS. Performance analysis of modified wavelet difference reduction methods in image compression and transmission. International Journal of Advanced and Applied Sciences. 2023; 10(10), Pages: 229-238.
- [23] Viswanthan P, Kalavathi P. Subband Thresholding for Near-Lossless Medical Image Compression. International Journal of Computing and Digital Systems. 2023; 14(1), 1-1.
- [24] Ahamad MG, Almazyad A, Ali SA. Design and development of new parametric wavelet for image denoising. International Journal of Electronics and Communication Engineering. 2011; 4 (1), pp.1-9
- [25] Da Silva PCL. Use of daubechies wavelets in the representation of analytical functions. In Wavelet Theory. IntechOpen. 2020.
- [26] Ince IF, Bulut F, Kilic I., Yildirim ME, Ince OF. Low dynamic range discrete cosine transform (LDR-DCT) for high-performance JPEG image compression. The Visual Computer, 2022;38(5), pp.1845-1870.
- [27] Bulut F. Huffman Algoritmasıyla Kayıpsız Hızlı Metin Sıkıştırma. El-Cezeri, 2016; 3, no. 2.